

**MULTI-SCALE QUANTITATIVE ASSESSMENT OF APOPTOSIS, BIOENERGETICS,
AND OXIDATIVE STRESS MOLECULAR MECHANISMS IN THE SOD1
G93A TRANSGENIC ALS MOUSE MODEL**

A Thesis
Presented to
The Academic Faculty

by

Kenneth Zhang

In Partial Fulfillment
of the Requirements for
Research Option in the
Department of Biomedical Engineering

Georgia Institute of Technology
May 2017

**MULTI-SCALE QUANTITATIVE ASSESSMENT OF APOPTOSIS, BIOENERGETICS,
AND OXIDATIVE STRESS MOLECULAR MECHANISMS IN THE SOD1
G93A TRANSGENIC ALS MOUSE MODEL**

Approved by:

Dr. Cassie Mitchell
Department of Biomedical Engineering
Georgia Institute of Technology

Signature: _____

Date Approved: _____

Dr. Melissa Kemp
Department of Biomedical Engineering
Georgia Institute of Technology

Signature: _____

Date Approved: _____

TABLE OF CONTENTS

	Page
ACKNOWLEDGEMENTS	5
LIST OF TABLES	6
LIST OF FIGURES	6
ABSTRACT	7
<u>CHAPTER</u>	
1 INTRODUCTION	8
2 MATERIALS AND METHODS	10
2.1 Data Collection and Inclusion	10
2.2 Aggregation Scheme	10
2.3 Direct Statistical Analysis of Aggregated Experimental Data	11
2.4 Computer Model Simulation with Dynamic Meta-Analysis	12
3 RESULTS: STATISTICAL COMPARISON OF EXPERIMENTALLY ASSESSED REGULATORY RESPONSE IN SOD1 G93A ALS AND WILD TYPE MICE	16
3.1 Apoptosis, Bioenergetics, and Oxidative Stress are Highly Interrelated	16
3.2 Elevated Level of Apoptosis- and Oxidative Stress-Related Parameters Observed in SOD1 G93A Mouse Model	16
3.3 Temporal Trends in Apoptosis, Bioenergetics, and Oxidative Stress-Related Parameters Decrease Over Time in SOD1 G93A Mouse Model	19
3.4 SOD1 G93A and Wild-type Mouse Model Elicit Markedly Different Responses to Perturbations	21
3.5 Cell Viability of SOD1 G93A Mouse Model Significantly Affected by Apoptosis- and Oxidative Stress-Related Perturbation <i>in vitro</i>	22
3.6 Contributions of Observed Data Variance <i>in vitro</i> and <i>in vivo</i>	23

4	RESULTS: DYNAMIC META-ANALYSIS COMPUTER SIMULATION OF SYSTEM REGULATION IN SOD1 G93A ALS AND WILD TYPE MICE	24
4.1	Construction of Dynamic Meta-Analysis Models	24
4.2	Genetic Algorithms Generates Distinctive Solution Sets for Wild Type Mouse	26
4.3	Gain Matrices from Genetic Algorithms Reveals High Degree of Degeneracy	27
4.4	Cross Correlation between Parameters of Wild-type Mouse Model <i>in vitro</i> and <i>in vivo</i>	29
4.5	Future Directions	30
5	DISCUSSION	31
5.1	Sensitivity of SOD G93A Mouse Model to Apoptosis- and Oxidative Stress-driven Changes to the System	32
5.2	Regulatory Mechanisms in SOD1 G93A and Wild-type Mice: A Comparison	39
5.3	Role of Bioenergetics-Apoptosis-Oxidative Stress Triad in ALS System Instability.	40
	REFERENCES	42

ACKNOWLEDGEMENTS

I wish to thank my teammates, Dhanushka Vitharana and Thao Nguyen Bach, for their collaboration in majority of the work, especially in statistical analysis. I also want to thank our technical team managers, Grant Coan and Renaid Kim, for providing help throughout different stages of this project.

LIST OF TABLES

	Page
Table 1: <i>In vivo</i> data count.	25
Table 2: <i>In vitro</i> data count.	25
Table 3: Average cross correlation from outputs of DMA model using 100 gains matrices generated by genetic algorithm.	29

LIST OF FIGURES

	Page
Figure 1: Relationship maps for aggregated metrics <i>in vivo</i> and <i>in vitro</i> indicate that the parameters within the apoptosis-bioenergetics-oxidative stress triad are highly interrelated.	17
Figure 2: Time-averaged and time-binned physiological parameter values reveal that primarily apoptosis- and oxidative stress-related metrics are elevated at various points in disease course in SOD1 G93A mice.	20
Figure 3: Temporal trends reveal that several SOD1 G93A metric levels decrease relative to WT levels over time.	26
Figure 4: Temporal trends of SOD1 G93A and WT treatment data reveal more dramatic oscillatory behavior in SOD1 G93A mice in response to perturbations than WT mice.	27
Figure 5: Perturbations to both SOD1 G93A and WT systems show significant changes <i>in vitro</i> .	28
Figure 6: Principal component analysis (PCA) of individual metrics in SOD1 G93A and WT mice.	35
Figure 7: Simulation of wild-type mouse model without optimization.	36
Figure 8: Simulation of wild-type mouse model using optimized gain matrix.	37
Figure 9: Boxplot of gain values from 1000 runs of genetic algorithm.	38

ABSTRACT

Apoptosis, bioenergetics, and oxidative stress have been implicated in Amyotrophic Lateral Sclerosis (ALS) disease progression; it is unclear as to how the interactions within this highly inter-related triad of categories influences the time course of the disease or, how effective therapeutic modulation could be accomplished. In this multi-scale study, we aim to simulate the molecular responses in ALS and map the timing of the interactions between the response mechanisms in high-copy SOD1 G93A (superoxide dismutase-1, glycine 93 to alanine) transgenic mice in order to determine which parameters and relationships have the most significant impact on ALS in each stage of the pathology. In addition, the possibility of homeostatic instabilities within the triad prior to, during, and after ALS symptom onset is examined. We observed several apoptosis- and oxidative stress-related metrics which are elevated throughout ALS disease course, with evidence of early disturbances. We identify regulatory differences within the apoptosis-bioenergetics-oxidative stress triad between G93A and wild type mice that could contribute to homeostatic instability leading to ALS symptom onset and disease progression.

CHAPTER 1

INTRODUCTION

Amyotrophic Lateral Sclerosis (ALS) is a fatal neurodegenerative disease characterized by the loss of motor neuron activities in the spinal cord, which leads to muscle paralysis, dysphagia, respiratory distress, and ultimately death. The causative mechanism of the disease has yet to be elucidated. Less than 10% of ALS cases are considered to be familial; the overwhelming preponderance are considered “sporadic” with no definitive known cause. [1] Several theories have been proposed regarding the possible etiology, which have been tested to varying extents using different transgenic *in vitro* and *in vivo* mouse models. The transgenic superoxide dismutase 1 glycine 93 to alanine mutation (hereafter referred to as SOD1 G93A) represents one of the most commonly used mouse models to study ALS pathophysiology [2]. In fact, the Laboratory for Pathology Dynamics at Georgia Institute of Technology has transcribed data from over 3,800 peer-reviewed articles for the SOD1 G93A mouse model.

Kim et. al, 2015 identifies multiple interrelated categorical disturbances contributing to ALS disease progression ranging from axonal transport to excitotoxicity. [3] Of these factors, apoptosis, bioenergetics, and oxidative stress have been identified as some of the key molecular mechanisms affecting ALS pathophysiology. In SOD1 G93A mice, mitochondrial respiration, specifically the electron transport chain, and ATP synthesis have been found to be impaired. [4] Furthermore, ATP has been implicated in neuromuscular junction (NMJ) damage through production of an inhibitory action on neurotransmitter release via reactive oxygen species (ROS) induction. [5] Oxidative stress is believed to increase the net production of ROS and reactive nitrogen species (RNS) and affect protein conformation and structure which can lead to the accumulation of abnormal protein inclusions. [6] In addition, several apoptotic factors have been implicated in ALS disease progression, such as the caspase family, notably in the pre-symptomatic and end-stages of the disease. [7]

Our lab has also previously developed the homeostatic instability theory, which states that several cellular or systemic perturbations have the ability to initiate a pathophysiological cascade resulting in homeostatic instability - the inability to maintain or restore homeostasis. [8-10] In the framework of this theory, ALS systems’ inability to efficiently and effectively utilize

regulatory mechanisms to compensate for instabilities results in the “ALS” phenotype.

The present study investigates the interactions within the apoptosis - bioenergetics - oxidative stress triad and examines their effect on ALS disease progression. In particular, we examine the possibility of instabilities in the SOD1 G93A model manifesting throughout disease progression through application of experimental perturbations. The hypothesis behind the present study is that system-level regulatory dysfunction could be driving ALS disease progression irrespective of the initiating causative perturbation. In fact, motoneurons, in general, are known to be more susceptible to instability [11]. To this end, we compare the regulatory responses of SOD1 G93A ALS mice to wild type mice. The long-term goal is to identify treatment targets that focus on re-establishing system stability, or homeostasis, after the clinical onset of ALS. Such an approach best considers the multi-factorial nature of ALS and is more likely to lead to therapeutic strategies that could help a greater portion of the ALS population, albeit whether the initiating etiology is familial, sporadic, environmental, or somewhere in-between.

The study consists of two major thrusts: 1) Statistical assessment of aggregated *in vitro* and *in vivo* experimental data from the apoptosis - bioenergetics - oxidative stress triad to assess the SOD1 G93A regulatory response, including magnitude and directionality of responses compared to wild type mice; 2) Dynamic meta-analysis computer simulation to examine system dynamics of the SOD1 G93A mouse model and parameter optimization to search for potential treatment targets that could re-establish homeostasis in ALS, corresponding to life-prolonging interventions or possibly even a cure.

The Methods utilized for both thrusts, including protocols for planned future work, is presented in Chapter 2. The work of the first thrust was completed and the results of the statistical assessment of experimental data is presented in Chapter 3. The second thrust, which included the construction of a multi-scalar dynamic meta-analysis computer simulation of both the SOD1 G93A and wild type mouse models, is a large undertaking that extends beyond the scope of the present thesis; Chapter 4 presents the results to date of the dynamic meta-analysis computer simulation as well as future plans to ultimately complete this portion of the work. Finally, Chapter 5 presents a Discussion of the findings to date and their implications for future work.

CHAPTER 2

MATERIALS AND METHODS

2.1 Data Collection and Inclusion

A literature review was performed to establish the scope of the study with particular focus on the triad of apoptosis, bioenergetics, and oxidative stress as the topics of interest. A set of keywords pertaining to these topics was compiled in order to assist in narrowing the data search. A PubMed search resulted in approximately 2000 relevant experimental articles for data extraction. The data pool for the study was compiled by only including results that contained quantifiable data from both *in vivo* and *in vitro* studies; in the current study, *in vivo* and *in vitro* data are analyzed separately. In addition, papers containing control and treated data for SOD1 G93A and wild-type mice were considered to ensure that the effects of different etiological perturbations could be quantified. Finally, treatments and experimentally assessed outcomes (i.e. referred to as “outputs”) in the data entries were only considered if they were direct measures of categories in the metrics list. The final data pool that satisfies all the inclusion criteria included more than 700 data points from 70 individual articles.

2.2 Aggregation Scheme

Collected data was assigned to a set of coordinates indicating a relationship, one coordinate for the perturbation and one coordinate for its measured effect. For relationships without sufficient numbers of data points to ensure statistical significance, an aggregation scheme was developed to pool similar metrics together; metrics were grouped based on their pathophysiological functionality.

- a) *Apoptosis*: All parameters directly relating to or leading to programmed cell death were listed under this category. Furthermore, metrics measuring necrotic cell death, unspecified cell death, and cell viability are also listed under this category.

The outputs in this category were:

- (1) *Pro-apoptotic factors*: caspases, cytochrome C release, etc.
- (2) *Anti-apoptotic factors*: Bcl-2, zVAD-fmk, etc.
- (3) *Cell Death*: both necrotic and apoptotic cell death

- (4) *Cell Viability*
- b) *Oxidative Stress*: All parameters relating to the production of free radicals and antioxidants.
- The outputs for this category were:
- (1) *SOD1 levels*: SOD1 enzymatic activity, function
 - (2) *Pro-oxidative stress factors*: free radicals, ROS, etc.
 - (3) *Antioxidants*: glutathione levels, free radical scavengers, etc.
 - (4) *Oxidative stress damage*: oxidative damage to protein, lipids and DNA
- c) *Bioenergetics*: All parameters relating to different cellular processes that harvest and transform energy such as cellular respiration and other metabolic processes that lead to the production and utilization of energy.
- This category's outputs were:
- (1) *Energy consumption*: oxygen consumption, ATP levels, glucose levels, etc.
 - (2) *Energy production*: activities of complexes in the electron transport chain, ADP levels, etc.

2.3 Direct Statistical Analysis of Aggregated Experimental Data

The fold changes of the experimentally assessed outcome metric in SOD1 G93A mice and WT mice were recorded and expressed as a normalized metric for each study or study aggregate using the ratio of the SOD1 G93A / WT. Comparisons included observations of the ratio of untreated transgenic and wild type mice (untreated SOD1 G93A / untreated wild type) as well as observations of the responses of treated transgenic and wild type mice (treated SOD1 G93A response / treated wild type response). "Treated" (i.e. perturbed) transgenic and wild type mice were used to assess possible differences in the rate of regulatory response in SOD1 G93A mice compared to wild type regulatory response. The resulting ratios were plotted versus time to examine the magnitude, directionality and rate of change in response to treated (i.e. perturbed) parameters. Observations were made both across the lifetime of the mice (in vivo) or the experimental time (in vitro). In the case of temporally binned data (when applicable), data samples were equally distributed.

Without making parametric assumptions about the collected data, linear regression was performed on the raw ratios to determine overall trends. Some linear regression lines were found

to have an imperfect fit due to the variations in data, and thus smooth curves were generated using locally weighted regression on Igor Pro. In addition, the ratios of the SOD1 G93A gain to the WT gain are expressed as mean \pm standard deviation. The Shapiro-Wilks test was used to determine the experimental data distribution, which was found to exhibit a non-normal distribution pattern. As such, the Kruskal-Wallis test was chosen as the primary statistical assessment due to its known superiority in statistically assessing a non-normal distribution. Significant differences in the magnitude of the responses to different perturbations were assessed using a Kruskal-Wallis analysis of variance followed by a multiple comparison test. A p-value of less than 0.05 was considered to be statistically significant. In addition, a principal component analysis (PCA) was performed on the transformed individual metric data to determine which metrics were responsible for producing the largest variance. All statistical tests were conducted using MATLAB R2014a software.

2.4 Computer Model Simulation with Dynamic Meta-Analysis

Our lab previously developed a mathematical modeling method called dynamic meta-analysis (DMA) to simulate temporal changes and dynamics of progression of multi-factorial pathologies, including ALS. [7] Unlike traditional meta-analysis, which requires a “static” assumption (i.e. does not include time), dynamic meta-analysis predicts responses of the outputs of interest to different perturbations over time by incorporating time-varying interactions between parameters. The model consists of a list of initial values for the parameters being simulated and a gain matrix both of which are discussed in detail in the following sub-sections. The output of the dynamic meta-analysis function for the present study is the values (i.e. ratios of perturbed responses over control responses) of each parameter over a specified time. We utilize maximum lifespan of the SOD1 G93A mouse (200 days for in vivo and 100 days for in vitro) for the simulated duration. Equation 1 describes the calculation performed at each time step of the model.

Equation 1.

$$[Outputs]_n = [Outputs]_{n-1} + [Outputs]_{n-1} \cdot ([Gain Matrix] * [Outputs]_{n-1})$$

In equation 1, n is each time step in days. At $n=1$, $[Outputs]_{n-1}$ is equal to a vector of initial values for all the parameters. Due to different life spans of *in vivo* and *in vitro* experimental models, *in vitro* data were run separately from *in vivo* data, with the same amount of time steps performed for each parameter.

2.4.1 Construction of the computational model gain matrix

As part of the calculation shown in Equation 1, DMA utilizes a gain matrix, which contains the average daily gain for every simulated parameter. The gain is analogous to a feedback gain in engineering control theory, which specifies how the rate and magnitude of change associated with one output will impact the response of a related output. In order to capture the gain for each output, the gain was calculated from the raw experimentally measured ratio of treated over control at discrete experimentally measured points of time. Gains at discrete experimentally measured time points are transformed into a continuous function which calculates the gain at each day of the *in vivo* or *in vitro* experimental model lifespan. Where applicable, the average of the time-vary gains for each categorical parameter (e.g. caspase, cytochrome c, etc.) is used to determine the aggregate time-varying gain for the category (e.g. pro-apoptosis). The ratio in Equation 2 represents the ratio of the SOD1 G93A gain to the WT gain (SOD1 G93A gain / WT gain).

$$\text{Equation 2. } Gain = average(\overset{days}{\sqrt{ratio}})$$

2.4.2 Optimizing parameters to construct a stable or “homeostatic” wild type mouse model

Due to the lack of published data for certain relationships, the gain matrices of both SOD1 G93A and wild-type mouse models contain empty values. Without these values, neither the SOD1 G93A or wild type model emulates expected regulation. In particular, it is assumed that the outputs of the wild type mouse should be stable over time, due to its ability to compensate for transient perturbations and ultimately maintain homeostasis. Without a homeostatic wild type mouse model, regulatory changes in the SOD1 G93A mouse cannot be

fully evaluated. Thus, we utilize a search-survey-summarize approach [9] to find appropriate values to insert into the empty gain matrix cells, which should theoretically provide the regulatory feedback needed to enable wild type mouse homeostasis (i.e. output stability over the normal life span of the wild type mouse).

In this study, a genetic algorithm from Matlab's global optimization toolbox was used to optimize the empty values in the wild-type gain matrix. Compared to other search methods such as Simplex search, genetic algorithms have the advantage of generating a large amount of solution sets across all regions using "parent seeds". Thus, it does not require an acutely accurate initial guess, which would otherwise be difficult to determine due to lack of corresponding experimental assessments in the physiological literature.

Genetic algorithm parameter optimization was utilized to find missing gain values that result in wild type mouse outcome stability upon reaching steady state. To assess the stability of each of the optimized gain matrices generated from the genetic algorithm, eigenvalues were calculated using Matlab. If all the eigenvalues have real parts that are negative, the steady state of the system is considered to be stable. In addition, if an eigenvalue has a real part that equals zero and is not complex, it is considered the same as having a negative real part (i.e. it is a stable solution). For any other permutations of eigenvalues, the system is considered to be unstable at steady state. As a starting point, 1,000 degenerate solution sets were generated by the genetic algorithm.

The degenerate solution sets were quantitatively and qualitatively evaluated to determine which of the parameter ranges could be physiologically relevant in the wild type mouse. Parameter sensitivity analyses (e.g. altering an individual parameter by a set percentage and re-running the model to assess effect) of both optimized parameters and initial start values of the outputs were used to quantify impact. Other analyses include visualization of the relationships among optimized parameter sets and corresponding outputs using cross-correlation analysis, box plots, and standard heuristic or pattern-determining assessments (e.g. time constant of steady state, amplitude of highest non-steady state peak, etc.). Where possible, experimental literature was used to determine possible boundaries of optimized parameter ranges or initial output start values. Finally, the simulated temporal outputs (or outcomes) corresponding to the identified

potentially physiologically relevant parameter solution sets were compared to known physiological outcomes at discrete time points with data not used to construct the model.

2.4.3 Protocol for constructing SOD1 G93A computational model with full gain matrix

The SOD1 G93A gain matrix is missing the same empty gain matrix values as the wild type. Therefore, once the missing values from the wild type gain matrix have been determined, they were directly inserted into the SOD1 G93A gain matrix. Unlike the wild type mouse, we cannot assume that the SOD1 G93A mouse is stable, especially post-onset. Thus, with the presently existing experimental data, there is no way to truly “optimize” the SOD1 G93A equivalent of the optimized wild type missing values. However, the insertion of the optimized missing wild type values into the base SOD1 G93A model allows a direct comparison of the differences between the known experimentally measured gain values and their impact on the corresponding SOD1 G93A system regulation and model outputs. Moreover, reverse engineering of SOD1 G93A stability (after ALS onset) through optimizing either the missing gain values or the known experimentally determined gains provides the equivalent of theoretical ALS treatments. The same genetic algorithm as used for optimizing the wild type model can be utilized to reverse engineer ALS post-onset stability in the SOD1 G93A ALS model by searching for the gain modifications needed to establish post-onset stability. Modified gains necessary to re-establish stability in the SOD1 G93A ALS model become possible treatment targets.

CHAPTER 3

RESULTS:

STATISTICAL COMPARISON OF EXPERIMENTALLY ASSESSED REGULATORY RESPONSE IN SOD1 G93A ALS AND WILD TYPE MICE

3.1 Apoptosis, Bioenergetics, and Oxidative Stress are Highly Interrelated.

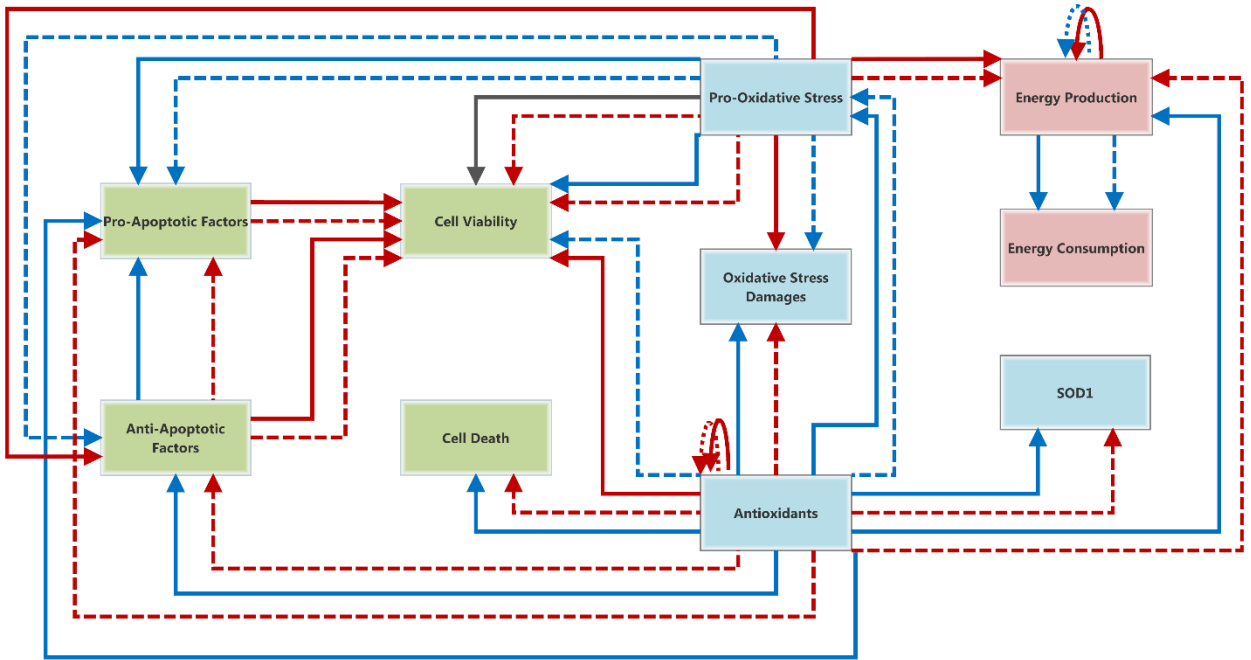
Figure 1 presents densely connected relationship maps for the *in vitro* and *in vivo* models. In total, 21 relationships were identified *in vitro* and 20 relationships were observed *in vivo*. Qualitative examination of the relationships illustrates that metrics belonging to apoptosis, bioenergetics, and oxidative stress are highly interrelated. Notably, the majority of the relationships were between apoptosis- and oxidative stress-related metrics. Given the sheer number of relationships observed involving oxidative stress- and apoptosis-related metrics, these categories appear to be more interactively contributing to ALS disease progression than bioenergetics-related metrics.

3.2 Elevated Levels of Apoptosis- and Oxidative Stress-related Parameters Observed in SOD1 G93A Mouse Model.

Several studies have found links between elevated oxidative stress levels and ALS as a result of factors such as protein carbonyls, 3-nitrotyrosine, and oxidative damage, which have been found in increasing levels in various tissues in ALS cases. [12] Through examination of the time-averaged control *in vivo* ratios, cell death levels were highest, followed by pro-oxidative stress factors, oxidative stress damages, SOD1, anti- and pro-apoptotic factors, and antioxidants. In particular, metrics pertaining to apoptosis or oxidative stress were present in higher levels, on average, throughout the disease course in SOD1 G93A mice. Interestingly, anti- and pro-apoptotic factor levels were the same, as well as energy production and consumption levels, suggesting that they dynamically balanced.



A.



B.

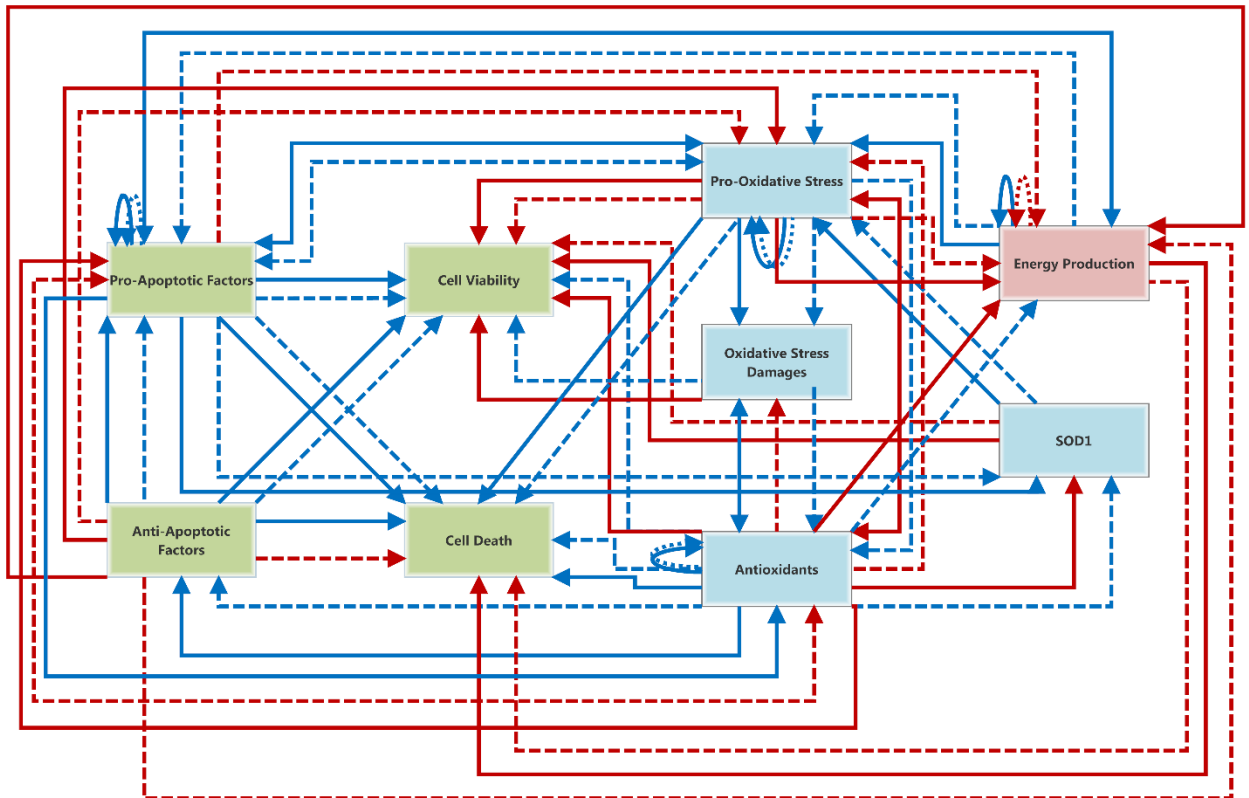


Figure 1. Relationship maps for aggregated metrics (A) *in vivo* and (B) *in vitro* indicate that the parameters within the apoptosis-bioenergetics-oxidative stress triad are highly interrelated. Relationships between parameters were identified and then classified based on the metrics table. The metric at the beginning of the arrow is defined as the perturbation and the metric at the arrowhead is defined to be the response. A positive correlation refers to when there is an increase in the response with respect to time; a negative correlation is observed when there is a respective decrease in the response. Most of the relationships observed are between aggregated metrics in the oxidative stress and apoptosis categories and more relationships were observed *in vitro* than *in vivo*. *A.* Oxidative stress-related metrics are primarily responsible for eliciting different responses in metrics. SOD1 G93A and WT mice respond in different ways to perturbations respond in opposite ways to perturbations from primarily oxidative stress-related metrics. Pro-oxidative stress factors caused a decrease in cell viability in SOD1 G93A mice, but no change in WT mice. Perturbations from antioxidants led to opposite trends observed in energy production, SOD1, oxidative stress damage, pro-oxidative stress, and cell viability levels in SOD1 G93A and WT mice. *B.* Similar to *in vivo*, oxidative stress-related metrics produce a variety of responses for metrics in SOD1 G93A and WT mice. Opposite responses were observed in SOD1 G93A and WT mice, primarily in response to antioxidants.

The results from the *in vitro* studies exhibit similar trends to the *in vivo* results, with pro-apoptotic factors, cell death, and oxidative stress damages having the highest levels. Similarly, these observations suggest that apoptosis- and oxidative stress-related metrics are present in larger amounts in SOD1 G93A mice than WT mice. Cell death levels remained elevated, however, and unlike the *in vivo* study, pro- and anti-apoptotic factors were not present in the same amounts. This finding implicates a major difference between the regulatory dynamics in *in vitro* and *in vivo* SOD1 G93A ALS models, which will ultimately need to be reconciled.

Levels of pro-oxidative stress factors, such as hydroxyl radicals, have been found to be greater in SOD1 G93A mice than in WT mice. [13] Examination of the temporal trends in the *in vivo* model revealed that cell death, oxidative stress damage, and pro-oxidative stress factors were elevated in SOD1 G93A mice at multiple points throughout disease progression. In addition, metrics classified under the oxidative stress category were elevated between 50 and 100 days in the *in vivo* model, encompassing pre-onset and onset of ALS (80 days). [11] Specifically, pro-oxidative stress values increased between 0-50 and 50-100 days, but plateaued beyond 100 days. Oxidative stress damage levels steadily increased during each time bin. These trends suggest that oxidative stress could be affecting disease progression as early as in the pre-onset stage and levels continue to remain high throughout the course of the disease.

While the time-averaged results suggested that overall, pro-apoptotic factor levels were higher in SOD1 G93A mice, they actually decreased between 50-100 and post 100 days *in vivo*.

In addition, cell death levels were elevated between 0-50 days and post 100 days. Given the greater levels of cell death, the decrease in pro-apoptotic factors could suggest that cell death may not have been induced through apoptotic pathways, but rather through other forms of cell death such as necrosis.

The *in vitro* model displays similar trends in that apoptosis- and oxidative stress-related metrics were also elevated throughout the disease course of SOD1 G93A mice. Apoptosis levels in SOD1 G93A mice were higher than WT levels throughout disease progression; metric levels peak between 1 and 2 days, and then decrease. Oxidative stress metric levels are considerably lower than apoptosis-related metrics. Once again, comparison of the specific trends observed conflict with those observed in the *in vivo* model. *In vitro* cell death in SOD1 G93A mice, while still elevated above WT levels, decreased with each successive time step. Trends in pro-apoptotic factors in the *in vitro* model, however, were consistent with those observed in the *in vivo* model in that pro-apoptotic factors decreased with time.

3.3 Temporal Trends in Apoptosis, Bioenergetics, and Oxidative Stress-related Parameters Decrease Over Time in SOD1 G93A Mouse Model.

SOD1 G93A *in vitro* levels of antioxidant, cell viability, and energy production relative to WT decreased with time. (Fig. 3A) Evaluation of the levels of these metrics reveals that SOD1 G93A antioxidant levels were initially greater than WT levels and both SOD1 G93A energy production and cell viability levels were lower than WT levels. These physiological occurrences suggest that not only does the disease affect how SOD1 G93A mice are able to respond to perturbations or changes to their physiology, as exemplified by the decrease in cell viability and energy production, but also suggests that initial levels of these factors are pre-emptively different in SOD1 G93A mice compared to WT mice. Thus, the SOD1 G93A ALS mice have some *de facto* differences in their physiology that are present at birth, well before the onset of functionally visible ALS symptoms.

In SOD1 G93A mice, reductions in mitochondrial respiration have been found to be linked to oxidative stress in the spinal cord. [14] The results indicate that SOD1 G93A *in vivo* levels of pro-apoptotic and energy production levels decreased with respect to WT mice, but oxidative stress damage levels increased. (Fig. 3B) The *in vivo* trend in energy production is consistent with the trend observed *in vitro*. Furthermore, trends in pro-apoptotic factors and

oxidative stress damage were consistent with the results obtained in Figure 2 as they decreased and increased, respectively, with time.

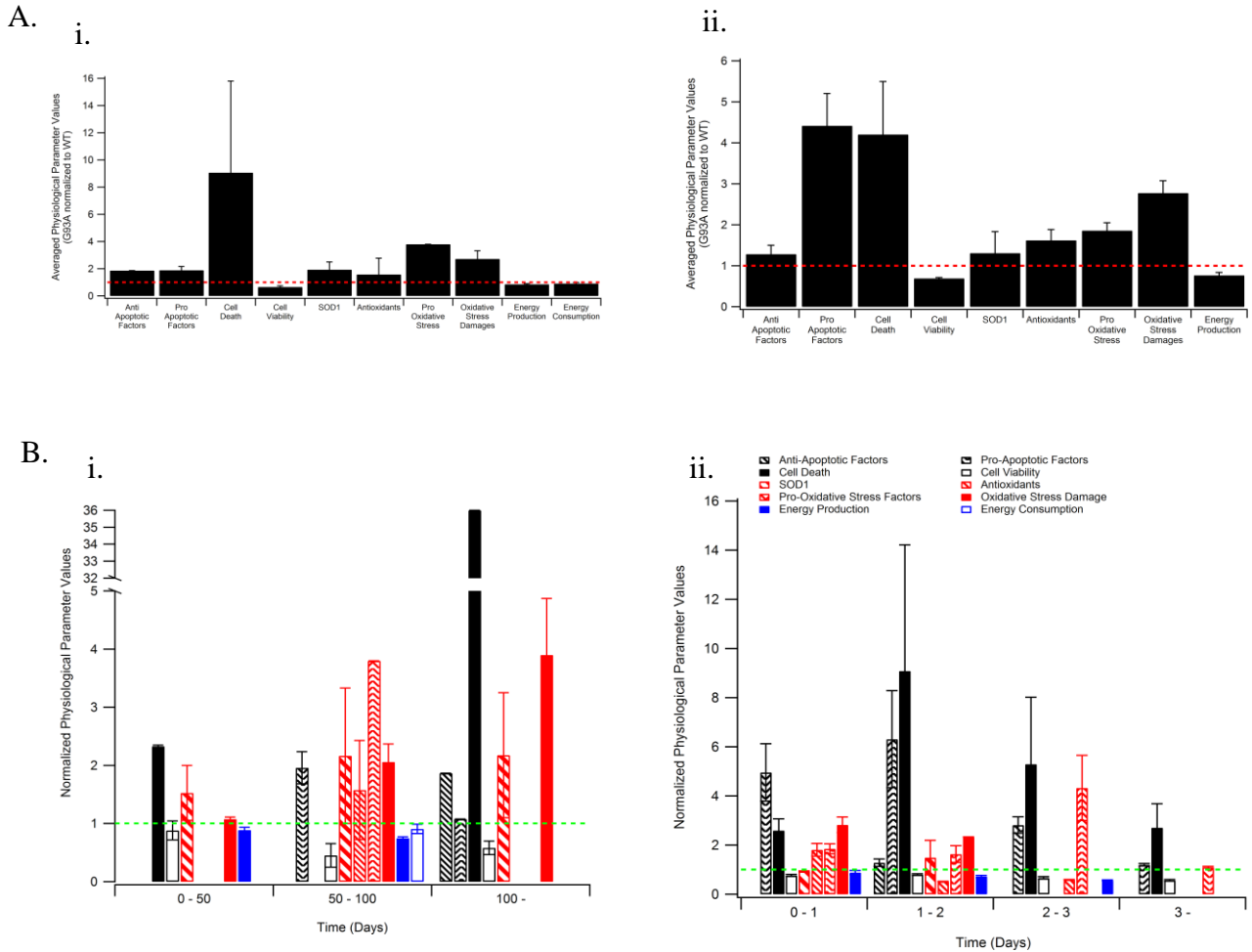


Figure 2. Time-averaged and time-binned physiological parameter values reveal that primarily apoptosis- and oxidative stress-related metrics are elevated at various points in disease course in SOD1 G93A mice. SOD1 G93A control data were normalized to their corresponding WT control data. **A.** Control ratios for SOD1 G93A and WT mice show elevated levels of apoptosis- and oxidative stress-related metrics both *in vivo* (i) and *in vitro* (ii). (i). Pro- and anti-apoptotic factor levels, as well as energy production and energy consumption levels, have similar levels. Cell death has the highest observed value. (ii). Pro-apoptotic factor and cell death levels are elevated, as well as oxidative stress damage levels. **B.** Fold changes in aggregated physiological metrics over time in *in vivo* (i) and *in vitro* (ii) models. Control ratios organized into different time bins revealed specific trends in the aggregated metrics. (i) Oxidative stress damage, pro-oxidative stress, and cell death levels are elevated at various stages throughout disease progression, and energy production and pro-apoptotic factor levels decrease during disease progression. (ii) Apoptosis-related metrics are present in larger amounts throughout disease progression.

3.4 SOD1 G93A and Wild-type Mouse Model Elicit Markedly Different Responses to Perturbation.

A common theme emerging in this analysis is the notable differences between the SOD1 G93A and WT's physiological responses to perturbations, specifically the pronounced reactions from the SOD1 G93A mouse. These responses from each mouse type can be classified by their directionality (e.g. same or opposite directional response) and their response magnitude (e.g. larger or smaller absolute response). In addition, evidence of oscillatory behavior in response to perturbation was observed in both WT and SOD1 G93A mice, with SOD1 G93A responses having larger peak oscillation amplitudes.

A relationship of particular interest was observed between oxidative stress damage and cell viability *in vitro* where the SOD1 G93A and WT systems produced opposite reactions in response to the perturbation. (Fig. 4Ai) Cell viability in the SOD1 G93A *in vitro* system considerably increased with the presence of oxidative stress damage, whereas cell viability in the WT system minimally decreased. Examination of the slopes of each line indicates that the slope of the SOD1 G93A response is 90 times the slope of the WT response. This observation is in contradiction with literature results as oxidative stress damage has been found to decrease cell viability.

In many cases, the SOD1 G93A mouse responds more dramatically to perturbations than the WT mouse, producing a greater magnitude of change in its response. Oxidative stress damage caused an increase in antioxidant levels in both SOD1 G93A and WT mice *in vitro*, however, the magnitude of change in the SOD1 G93A response was almost three times higher than WT response. (Fig. 4Aii) In addition, large oscillations were observed early on in the disease course suggesting that the SOD1 G93A system is particularly sensitive to oxidative stress damage. It is also important to note that initial antioxidant levels in the SOD1 G93A system were already elevated above WT levels, indicating that there are initial differences between the two mouse types at the cellular level even prior to full ALS onset. The application of antioxidants to both the SOD1 G93A and WT systems *in vivo* led to an overall decrease in oxidative stress damage despite an initial spike following the perturbation. (Fig. 4Bi) The change in oxidative stress damage levels was five times as great in SOD1 G93A mice as it was in WT mice. In addition, application of antioxidants led to initial fluctuations in levels of SOD1 G93A cell

viability and an overall decrease in cell viability *in vitro* (Fig. 4Bii). Overall, the WT physiology was largely unaffected by the increase in antioxidant levels and exhibited oscillations with small amplitudes. These results suggest that the SOD1 G93A physiology is more sensitive to antioxidant perturbations, which results in large oscillations. In contrast, the WT physiology is robust and can ultimately re-stabilize to internal or external perturbations.

The combination of these observations indicates that the SOD1 G93A system is responding more aggressively to perturbations and could point to underlying instabilities in the regulatory mechanisms. Furthermore, the nature of the WT responses suggest that the system is generally unaffected by perturbations. Thus, the WT system could be utilizing compensatory mechanisms that are either simply not present or perhaps dysfunctional in the SOD1 G93A system.

3.5 Cell Viability of SOD1 G93A Mouse Model Significantly Affected by Apoptosis-and Oxidative Stress-related Perturbation *in vitro*.

After performing a Kruskal-Wallis test using $p < 0.05$ and $p < 0.01$ to identify quantitative statistical significance, no significant results were observed *in vivo*. However, qualitatively, antioxidants produced the greatest increase and pro-oxidative stress factors the greatest decrease in SOD1 G93A cell viability, respectively.

Comparison of the effects of perturbations from apoptosis- and oxidative stress-related factors led to the most noteworthy results *in vitro*. Pro-apoptotic factors produced twice as large of a fold change in SOD1 G93A cell viability than pro-oxidative stress factors (Fig. 5A). Further analysis of the fold changes revealed that pro-apoptotic factors increased cell viability in the SOD1 G93A *in vitro* model whereas pro-oxidative stress factors actually decreased cell viability in SOD1 G93A *in vitro* model. Based on the SOD1 G93A responses to each of these corresponding perturbations, pro-oxidative stress factors negatively impacted *in vitro* SOD1 G93A cell viability whereas pro-apoptotic factors improved *in vitro* SOD1 G93A cell viability. Moreover, perturbations resulting from antioxidants significantly increased *in vitro* SOD1 G93A cell viability by approximately 1.5 times more than pro-oxidative stress factors (Fig. 5A). The marked increase in *in vitro* SOD1 G93A cell viability upon application of antioxidants could be indicative of an antioxidant deficiency in the *in vitro* SOD1 G93A experimental mouse model. Finally, oxidative stress damage led to a fold change of approximately 1.6 times more in *in vitro*

SOD1 G93A cell viability than pro-oxidative stress factors. (Fig. 5A) Since oxidative stress damage is caused by pro-oxidative stress factors, it is possible that oxidative stress damage did not have the ability to further “propagate”; thus, the damage to SOD1 G93A cell viability was capped due to the collinearity between pro-oxidative stress factors and oxidative stress damage.

3.6 Contributions of Observed Data Variance *in vitro* and *in vivo*.

Principal component analysis (PCA) illustrates which variable contributions are primarily contributing to outcome variance. We performed PCA on the aggregated, *in vitro*, and *in vivo* data sets. In both SOD1 G93A and WT *in vitro* responses, caspase-8 was the primary factor contributing to the variance observed (Fig. 6A, B). Caspase-8 is a protein involved in apoptosis induced by Fas and other apoptotic stimuli [15]. Specifically, caspase-8 is activated by death receptors, such as Fas and p75, which in turn activates executioner caspases using both direct and indirect methods through Bid. In WT mice, copper (an antioxidant as well as a key enzymatic catalyst) was the second-most important contributor to the variance in the data whereas, in SOD1 G93A mice, the pro-oxidative stress factors, iNOS and nNOS, were the second-most important contributor to variance. In both WT and SOD1 G93A *in vivo* responses, other antioxidants primarily contributed to the variance observed in the data (Fig. 6C-D) Ultimately, these results suggest that apoptosis- and oxidative stress related metrics account the most for variance in both *in vitro* and *in vivo* WT and SOD1 G93A data, and conversely, bioenergetics contributes the least to observed variance.

CHAPTER 4

RESULTS:

DYNAMIC META-ANALYSIS COMPUTER SIMULATION OF SYSTEM REGULATION IN SOD1 G93A ALS AND WILD TYPE MICE

4.1 Construction of Dynamic Meta-Analysis Models

Dynamic meta-analysis computer models were successfully constructed in Matlab using the methods described in Chapter 2. Figure 1 and Table 1 illustrates the connectivity and relationships, respectively, used to construct the models. Architecture was created to simulate *in vitro* wild type, *in vitro* SOD1 G93A, *in vivo* wild type, and *in vivo* SOD1 G93A mouse models. A matrix was established to house the gains utilized for each respective model type. The 2-D matrix for each model type has rows and columns of the same length, enabling a potential relationship between every assessed category. However, a relationship to fill every cell in the matrix was not always available or able to be calculated from the experimental literature. An initial simulation of the *in vivo* wild type model using only the available experimentally obtained gains illustrated the need for additional [experimentally unavailable] gains in order to obtain steady-state system stability, or homeostasis, in the *in vivo* wild type mouse model. To this end, a genetic algorithm was used to identify the “missing” gain values in the 2-D matrix using eigenvalue steady-state stability criteria as described in Chapter 2. Optimization was repeated for both the *in vitro* and *in vivo* wild type models. Given the size and scope of the dynamic meta-analysis computational model project, the present thesis focuses on wild type mouse model construction and results while providing a protocol and underlying programming architecture for completing the equivalent SOD1 G93A computer model.

Table 1. *In vivo* data count.

	Data Points	Ratios	Papers
B-B	36	18	4
B-A	0	0	0
B-O	0	0	0
A-A	36	18	6
A-B	0	0	0
A-O	0	0	0
O-B	36	18	4
O-A	40	20	8
O-O	56	28	10
A	62	31	-
B	60	30	-
O	50	25	-
Overall	204	102	23

A = apoptosis, B = bioenergetics, O = oxidative stress.

Table 2. *In vitro* data count.

	Data Points	Ratios	Papers
B-B	2	1	1
B-A	14	7	4
B-O	6	3	1
A-A	106	53	13
A-B	8	4	2
A-O	18	9	5
O-B	6	3	2
O-A	270	135	28
O-O	78	39	13
A	310	155	-
B	16	8	-
O	142	71	-
Overall	508	254	47

A = apoptosis, B = bioenergetics, O = oxidative stress.

The genetic algorithm generated 1,000 new gain matrices for both *in vitro* and *in vivo* wild-type model. In Figure 3, the changes of each parameters were plotted using the original gain matrix. Most of the parameters are diverging over the lifespan of the mouse (200 days). However, using a gain matrix generated from the genetic algorithm, all parameters were able to reach a steady state, as shown in Figure 4. From a quick analysis of the trends and shapes of the of the plots from the 1,000 simulations of the genetic algorithm, no specific patterns have been identified at the time of this writing. Continued analysis is in progress to differentiate parameter values with their corresponding solutions using a variety of qualitative and quantitative analyses as presented the Methods of Chapter 2.

4.2 Genetic Algorithms Generates Distinctive Solution Sets for Wild Type mouse

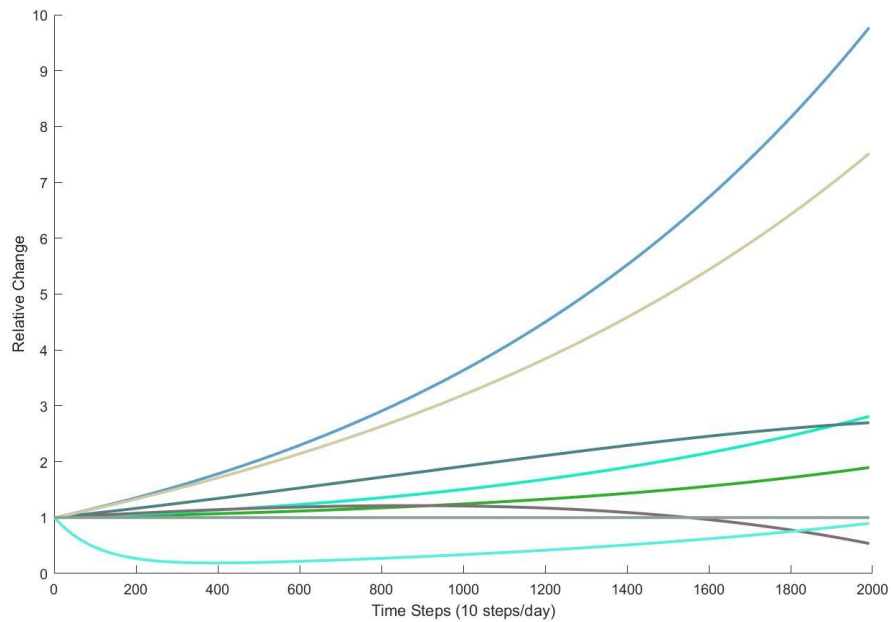


Figure 3. Simulation of wild-type mouse model without optimization. Parameters diverge over time, showing no signs of coming back to equilibrium.

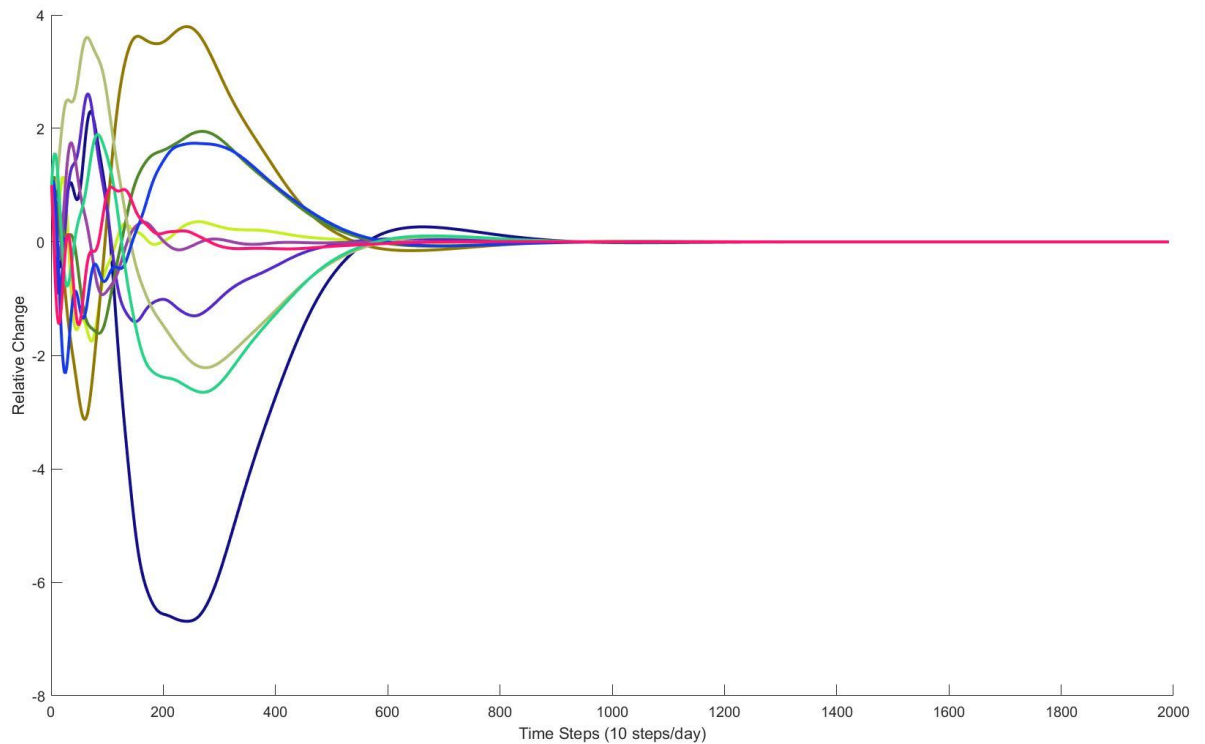


Figure 4. Simulation of wild-type mouse model using optimized gains matrix. System responds to perturbations and drives all parameters to an equilibrium.

4.3 Gain Matrices from Genetic Algorithms Reveals High Degree of Degeneracy

To analyze any similarities among the generated wild-type *in vitro* gain matrices, a boxplot, shown in Figure 5, was generated to show the span of each altered value. The plot illustrates a wide range of stable solution parameter values for almost all parameters, indicating that the stability or homeostasis of the wild-type system can be dependent on various distinctly different sets of parameter values. Thus, there is a high degree of degeneracy in the wild-type system with multiple pathways able to produce the same emergent property of homeostasis. The degree of degeneracy in the wild type mouse also hints that homeostatic instabilities in ALS could likely be caused by numerous individual or combinations of different factors. The boxplot indicates there is a substantial degree of stabilizing negative feedback terms (or gains), all of which belong to parameters of energy production, oxidative damage, pro-oxidative stress factors,

and cell viability. Since cell viability primarily serves as an output in our mathematical model, this result indicates that regulating energy production and oxidative stress levels are key to bringing wild-type mouse model back to steady state when the system experiences a perturbation. The latter result is particularly interesting given that, in the aggregated experimental data statistical assessment presented in Chapter 3, PCA reveals that bioenergetics accounted for the least amount of variance in the system. Likewise, energetics terms in the computational system had a narrower range of parameter values corresponding to stable system solutions. Collectively these results indicate a lesser degree of degeneracy with bioenergetics. The lesser degree of degeneracy with bioenergetics is likely tied to the lower number of inter-relationships between bioenergetics and other included metrics. It remains to be seen whether the present degeneracy or lesser inter-relatedness of bioenergetics will remain once additional categories of metrics are added (e.g. excitability, axonal transport, proteomics, etc.) On the other hand, the lesser degeneracy with bioenergetics could also be tied to the fact that measures of bioenergetics (e.g. ATP, respiration, etc.) are inherently lower in the SOD1 G93A ALS mice from birth, as presented in the previous chapter.

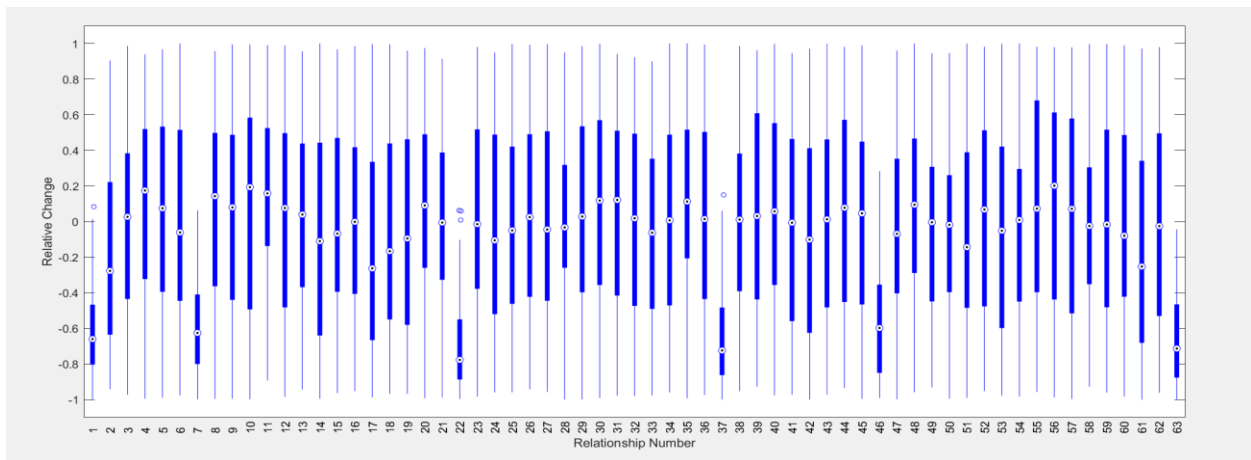


Figure 5. Boxplot of gains values from 1000 runs of genetic algorithm. Negative feedbacks are present in relationships 1, 7, 22, 37, 46, and 63, which all belongs to categories of energy production, pro-oxidative stress factors, and oxidative damage.

4.4 Cross Correlation between Parameters of Wild-type Mouse Model *in vitro* and *in vivo*

Sensitivity analysis with a 10-50% increase in each parameter were performed and the output's cross correlation with original outputs are calculated and the averages are shown in Table 3. Cell viability shows the least correlation to other parameters, which is a reasonable result because viability is often considered as an output or response in our model instead of a treatment or perturbation. In the biological system, cell viability could also be considered an emergent property. Inconsistency in *in vitro* and *in vivo* was seen in energy production, where it is highly correlated to other parameters *in vitro* and not *in vivo*. Oxidative stress damage has shown high correlation to other parameters both *in vitro* and *in vivo*. This high correlation may suggest that oxidative stress damage is a redundant parameter in the model. In fact, oxidative stress damage has a very similar classification as pro-oxidative stress factors. However, redundancy, like degeneracy, is expected and biological systems. Continued cross-correlation analysis, combined with heuristic assessments, will be applied as we seek to justify parameter values with physiological ramifications.

Table 3. Average cross correlation from outputs of DMA model using 1000 gains matrices generated by genetic algorithm. Values highlighted in green indicate relative high correlation, and red indicate relative low correlation.

<i>in vitro</i>										
	Energy Production	Energy Consumption	Cell Death	Anti-apoptotic Factors	Pro-apoptotic Factors	SOD1 Level	Antioxidants	Oxidative Stress Damage	Pro-oxidative Stress Factors	Cell Viability
Energy Production	0.978865631	0.982084474	0.981385502	0.977613629	0.983644787	0.97842804	0.981799907	0.982865401	0.985238055	0.980850773
Energy Consumption	0.971890291	0.97695565	0.97352935	0.974877196	0.974585542	0.970304445	0.97504205	0.97781029	0.978827458	0.976310474
Cell Death	0.974797296	0.972365948	0.978022394	0.973601371	0.979579079	0.972603295	0.981155065	0.970904286	0.978269885	0.967137418
Anti-apoptotic Factors	0.979285559	0.979577291	0.980610919	0.978220286	0.982665023	0.973586892	0.98166276	0.976056296	0.985534206	0.980360051
Pro-apoptotic Factors	0.96281418	0.96781095	0.967231049	0.967741207	0.966548309	0.967066971	0.9726347	0.967510456	0.965979356	0.961235048
SOD1 Level	0.970587922	0.967401627	0.974374061	0.975110186	0.97534099	0.964253433	0.981343651	0.977670219	0.976504717	0.979040018
Antioxidants	0.980334226	0.981320948	0.98114851	0.979439673	0.979408802	0.97859668	0.98120181	0.978417572	0.977790646	0.979468579
Oxidative Stress Damage	0.991352734	0.988246741	0.989044791	0.989203444	0.987574193	0.98796706	0.989704731	0.989592025	0.987201396	0.993283555
Pro-oxidative Stress Factors	0.972004109	0.976679823	0.971769323	0.975901787	0.972703439	0.96982938	0.970684573	0.972985743	0.979077374	0.972080215
Cell Viability	0.937872926	0.950631065	0.946842714	0.936197766	0.947641377	0.9477825	0.946873592	0.95178863	0.950577154	0.93477764
<i>in vivo</i>										
	Energy Production	Energy Consumption	Cell Death	Anti-apoptotic Factors	Pro-apoptotic Factors	SOD1 Level	Antioxidants	Oxidative Stress Damage	Pro-oxidative Stress Factors	Cell Viability
Energy Production	0.977864469	0.97797135	0.978761615	0.980138776	0.978999506	0.979107289	0.978262378	0.973285679	0.977675235	0.97816441
Energy Consumption	0.985355661	0.986763102	0.984829677	0.997926039	0.996318206	0.989889412	0.990441638	0.983436584	0.992480589	0.994917278
Cell Death	0.996568437	0.994490416	0.99717691	0.996966678	0.996448678	0.993199712	0.996961882	0.997201327	0.996023354	0.9966415
Anti-apoptotic Factors	0.995056693	0.995605867	0.997553484	0.99417816	0.99601155	0.993744016	0.997105806	0.9934626	0.99390672	0.99289357
Pro-apoptotic Factors	0.983544137	0.985472104	0.983645836	0.99635388	0.994534874	0.98864306	0.987972986	0.98243319	0.990739436	0.993084793
SOD1 Level	0.997730426	0.99727949	0.998262624	0.997908658	0.998332303	0.995991634	0.997863773	0.996410277	0.996429135	0.997168604
Antioxidants	0.988748159	0.987254857	0.990276319	0.976561078	0.978032413	0.981900842	0.985552009	0.988111876	0.979803872	0.978243853
Oxidative Stress Damage	0.99277009	0.994778737	0.996069679	0.991059898	0.985407016	0.989089409	0.996047132	0.988005636	0.994600617	0.991390281
Pro-oxidative Stress Factors	0.996542339	0.996081789	0.997089937	0.995853584	0.992431347	0.996222259	0.997631649	0.996653246	0.995146797	0.995941654
Cell Viability	0.977785077	0.973294394	0.976337569	0.980526523	0.98177638	0.979284246	0.976626469	0.975389157	0.971479988	0.975044357

4.5 Future Directions

The eventual goal of this study is to formulate a model that best describes the relationships among the factors involved in ALS pathophysiology. The current analysis on the wild-type gain matrices from genetic algorithm surely provides some insights on the underlying molecular mechanisms of ALS, but finding a specific wild-type gain matrix is necessary for further study on these mechanisms. Therefore, the next step of this project will be analyzing the current wild type gain matrices generated by the genetic algorithm, and identifying similarities among the matrices that can be supported by adjunctive physiological literature. Statistical analysis will be performed to set upper and lower limits for particular gains, thus narrowing the range of the potential physiologically relevant parameter values. Once a specific wild-type matrix is determined to be the best fit, simulations will be run that combine the experimentally determined SOD1 G93A gains with the overlapping “missing” gains optimized in the wild-type model. The simulation with SOD1 G93A data can be used as a tool to compare and contrast the effects of known differences in regulatory gains in the SOD1 G93A and wild type mice. Also, reverse engineering (as outlined in the Chapter 2 Methods) using genetic algorithm optimization can be used to search for possible treatments for ALS by identifying parameters (or gains) that can re-stabilize the SOD1 G93A system after the onset of visible ALS symptoms.

While the current models focus on the bioenergetics-oxidative stress-apoptosis triad, we plan to expand the model connectivity to include other pathophysiological categories known to contribute to ALS, such as axonal transport, inflammation, excitability, and proteomics. The aforementioned categories not currently included have functional endpoints that directly connect to the bioenergetics-oxidative stress-apoptosis triad. Thus, at present, the effects of these categories are implicitly included in the optimized “missing” gains analogous to a “blackbox” model contribution. Over-parameterization is a major concern in multi-scalar models. Thus, maintaining focus on the bioenergetics-oxidative stress-apoptosis triad, where the functional outcomes of ALS most directly result, was one way to initially avoid over-parameterization at this stage of the project.

CHAPTER 5

DISCUSSION

The present study identifies the relationships present within the apoptosis-bioenergetics-oxidative stress triad and reveals that the three categories are highly interrelated. The complexity of the interactions within the triad are underscored by the sheer number of relationships identified in Figure 1. There are many interacting variables in the G93A system, which in turn makes it difficult to isolate a single category, or factor, that can be implicated in ALS disease progression. It appears as if a combination of factors may be responsible, or minimally, a combination of factors may be required to treat ALS. Of the three categories studied, apoptosis and oxidative stress were more densely connected. Thus, their strong interactions suggest the possibility of exploiting synergistic relationships to treat mechanisms contributing to ALS progression. Several studies have implicated oxidative stress in inducing apoptotic cell death by triggering apoptotic pathways in the cell [12]. Specifically, oxidative stress damages, which cause injury to cellular components, trigger cell death [16]. While Bioenergetics does not have as strong of connections or as numerous interactions, the fact that bioenergetics is decreased throughout the lifespan of SOD1 G93A ALS mice (as illustrated in the Chapter 3 results), indicates it is an early precipitator of ALS progression. The narrower parameter ranges identified in the optimization of the wild type mouse dynamic meta-analysis computer model suggests there are less degenerate or redundant pathways to compensate for the effect of bioenergetics in maintaining homeostatic stability.

We hypothesize that the general principles behind system regulation could explain how a variety of different perturbation or initiating cellular events could evolve into the phenotype we see and know as ALS. The future ability to further assess and compare the system dynamics of SOD1 G93A ALS and wild type mouse through computer simulation will enable an assessment to determine what factors or feedback responses work sequentially, simultaneously, or a combination to produce the observed pathological system instability observed in SOD1 G93A mice. The nature of the interactions identified in the statistical analysis of aggregated experimental data as well as the dynamic meta-analysis computer simulations only reinforce that ALS is a complex, multifactorial disease.

5.1 Sensitivity of SOD1 G93A Mouse Model to Apoptosis- and Oxidative Stress-driven Changes to the System.

In Figures 2, 7, and 8, oxidative stress-related metrics were observed to be elevated during multiple time intervals throughout disease progression. Oxidative stress damages can lead to imbalances in ROS production and removal, which in turn causes ROS accumulation and can further exacerbate disease progression. [17] The increased presence of pro-oxidative stress factors and oxidative stress damage observed, especially in the early stages of the disease, suggest that the SOD1 G93A model is particularly sensitive to perturbation of these metrics. In literature, evidence of elevated oxidative stress factor levels prior to and at disease onset, has been found, which supports the findings of the present analysis. [18] Moreover, early signs of oxidative stress have been observed in all major neurodegenerative diseases, suggesting a common neuropathological continuum and perhaps even the possibility of shared therapeutic targets [19-21].

In addition, the SOD1 G93A model appears to be particularly sensitive to antioxidants. Multi-layer antioxidant networks are present in mitochondria to counteract oxidative stress damage, including internally produced oxidants of respiration as well as external exposure [22]. Deficiencies to the oxidative and anti-oxidative dynamic balance, for instance proteins (such as MnSOD) losing antioxidant function, can cause mitochondria to lose the ability to sufficiently compensate for oxidative stress damage. [22] Figure 6Aii highlights that SOD1 G93A control antioxidant levels decrease over time, suggesting that the SOD1 G93A model loses the capability to produce sufficient levels of compensatory antioxidants. Moreover, Figures 7Bi and 8A indicate that the addition of antioxidants decreases oxidative stress damage levels and increases cell viability in SOD1 G93A mice respectively, which is consistent with literature findings. [21] Figure 6Ai appears to contradict the present study's findings, as it suggests that treating SOD1 G93A mice with antioxidants actually decreases cell viability *in vivo*. One possible explanation for the previous observation could be that the SOD1 G93A model is utilizing a combination of mechanisms to compensate for the changes to the system and the addition of antioxidants leads to an excess in compensatory factors which ultimately has an adverse effect on cell viability. Alternatively, application of the antioxidant treatment could cause the SOD1 G93A model to overcompensate, which could partially destabilize the SOD1 G93A model. Both the experimental and computational results of this work do suggest that there is hyper-regulation or

overly aggressive responses to perturbation in the SOD1 G93A mouse model. Though meant to be helpful, it could be that the application of high levels of anti-oxidants in combination to the overly zealous SOD1 G93A regulatory response actually shifts the dynamic balance too far, from one of the spectrum to the other, resulting in harmful cell viability outcomes. Further investigation needs to be conducted to definitively elucidate the effect of antioxidants on disease progression. It appears the usage of anti-oxidants would have to be carefully tailored to the specific nature of temporal disease progression.

Furthermore, apoptosis-related metrics were observed to be elevated during various stages of disease progression. Apoptotic pathways trigger cell death, and removal of them has been associated with increased cell viability, motor function, and lifespan in familial ALS models. [19] Imbalances between pro- and anti-apoptotic factors in SOD1 G93A mice, which are elevated with respect to levels in WT mice, can be observed throughout disease progression both *in vitro* and *in vivo*. Cell death levels are also elevated. In regards to members of the Bcl-2 family, such as Bim, Bad, and Bax (all pro-apoptotic factors) and Bcl-2 (an anti-apoptotic factor), there is evidence that the ratio of anti- to pro-apoptotic factors influences the viability of developing and mature cells; considerable differences in levels of either factor can lead to activation of caspase-related apoptosis through release of cytochrome c into the cytosol. [23] In Figure 8A however, pro-apoptotic factor perturbations in fact increase SOD1 G93A cell viability, which is in direct contrast to literature findings. It is possible that the increase in pro-apoptotic factors could be inducing greater levels of death amongst unhealthy cells and thus preventing pre-existing damage, for instance from oxidative stress, from further propagating and decreasing healthy cell viability. Thus, the increase in pro-apoptotic factors could actually be a protective mechanism to prevent the “spread” of ALS. Again, the ability to dynamically balance pro- and anti-apoptotic factors is crucial. A recurring theme of the present work is that the SOD1 G93A mouse exhibits dynamic imbalances that complexly, rather than intuitively, influence the outcomes of the disease and its experimental markers. Dynamic imbalances point towards the need for carefully timed and titrated combination therapies to restore system-level homeostasis after the clinical onset of ALS symptoms.

Further analysis of the effect of apoptosis- and oxidative stress-related metrics on disease progression using PCA points to caspase-8, copper, iNOS/nNOS, other antioxidants, and other oxidative stress as major contributors to the trends observed. Specifically, the SOD1 G93A

model may be increasingly susceptible or over-active to perturbations relating to the bioenergetics-apoptosis-oxidative stress triad. For instance, literature findings suggest that SOD1 G93A motor neurons exhibit increased sensitivity to activation of the nitric oxide pathway downstream of Fas. [24] While cell death levels in SOD1 G93A and WT mice were comparable, SOD1 G93A produced more exaggerated cell death response even when perturbed with intermediate levels of Fas activation; as a result, the SOD1 G93A model was more sensitive to perturbations and an overexpression of WT SOD1 conferred protection against Fas-induced cell death. [24] Also, it should be noted that the experimentally observed levels of cell death in SOD1 G93A mice are likely under-represented since, as the disease progresses, there are simply less cells remaining in the SOD1 G93A mice compared to wild type. Therefore, at later stages of ALS, it may appear as if motoneuron cell death is a less of a factor when in reality most of the cells are already dead, and thus, additional cell death is difficult to assess.

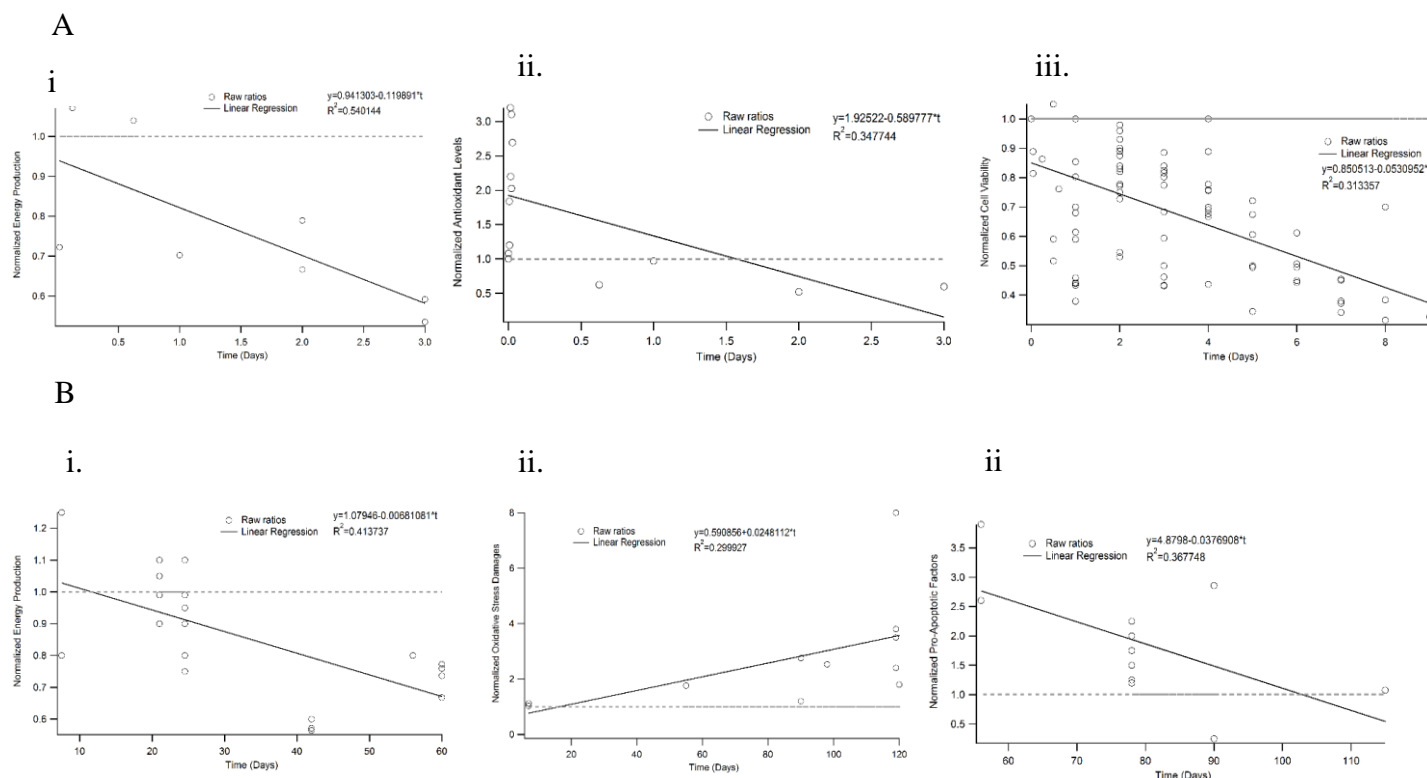


Figure 6. Temporal trends reveal that several SOD1 G93A metric levels decrease relative to WT levels over time. SOD1 G93A control data were normalized to their corresponding WT control data. *A.* Antioxidant, cell viability, and energy production levels all decrease with time *in vitro*. In SOD1 G93A mice, cell viability (iii) and energy production (ii) levels are initially depressed in comparison to WT levels, but antioxidant (i) levels are initially elevated. *B.* Pro-apoptotic factors (i) and energy production (ii) levels decrease with time and oxidative stress damage (iii) levels increase with time *in vivo*. In SOD1 G93A mice, pro-apoptotic factor and energy production levels are elevated in comparison to WT levels, but oxidative stress damage levels are initially lower. Linear regression was performed data to obtain the overall trend of the data.

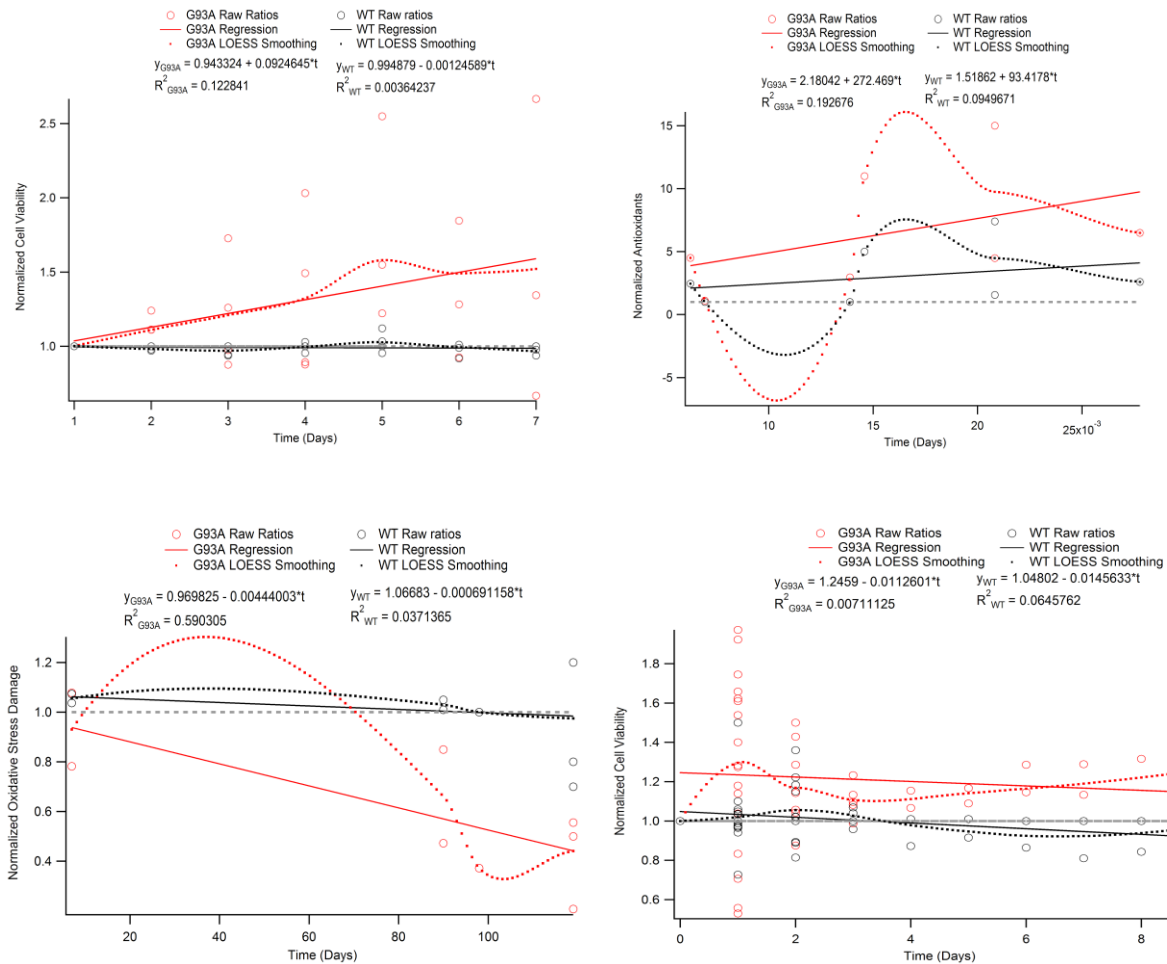


Figure 7. Temporal trends SOD1 G93A and WT treatment data reveal more dramatic oscillatory behavior in SOD1 G93A mice in response to perturbations than WT mice. SOD1 G93A treated data were normalized to their corresponding WT treated data. A. *In vitro* physiological responses. (i) SOD1 G93A and WT mice had opposite cell viability responses when perturbed with oxidative stress damage; SOD1 G93A cell viability levels increased, while WT cell viability levels decreased. (ii) Antioxidant levels increased in response to perturbations from oxidative stress damage in both SOD1 G93A and WT mice. SOD1 G93A antioxidant levels were considerably higher than WT antioxidant levels. B. *In vivo* physiological responses. Oxidative stress damage levels decreased, overall, in both SOD1 G93A and WT mice when perturbed with antioxidants; SOD1 G93A oxidative stress damage levels were lower than WT oxidative stress damage levels. Linear regression was performed data to obtain the directionality of the overall trend of the data, and a LOESS curve fitting was used to identify the specific trends in the data.

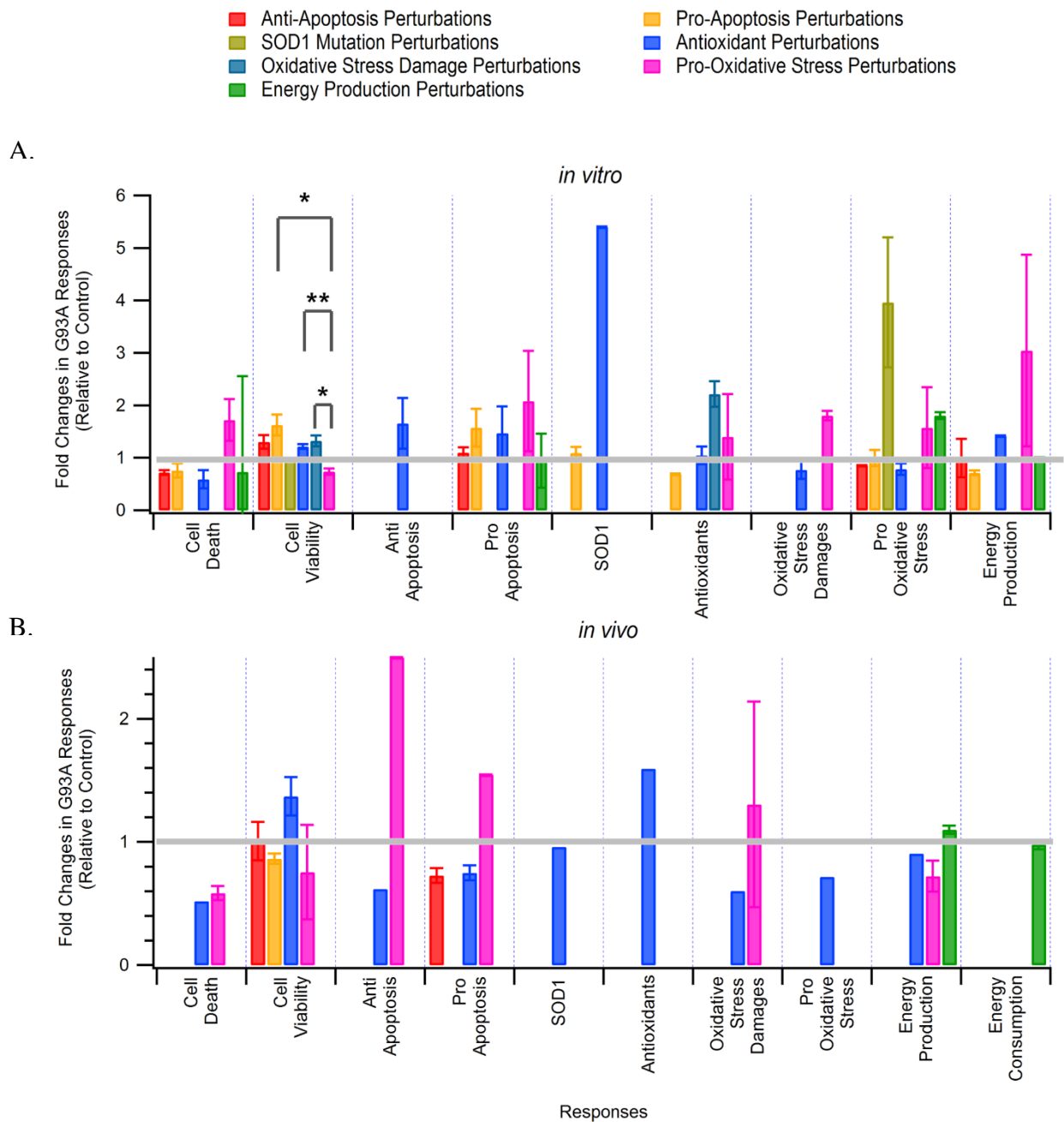


Figure 8. Perturbations to both SOD1 G93A and WT systems show significant changes in vitro. SOD1 G93A responses were normalized to WT responses in order to determine the fold change in response to the different perturbations belonging to the three broad categories of apoptosis, bioenergetics, and oxidative stress. Relationships with fold changes greater than one indicate that the SOD1 G93A system responds more dramatically to perturbations to the system than the WT system. (A) Fold changes in the SOD1 G93A responses to different perturbations in vitro. Most of the significant fold changes observed were between metrics belonging to apoptosis and oxidative stress. (B) Fold changes in the SOD1 G93A responses to different perturbations in vivo. No significant relationships were observed amongst metrics. Kruskal-Wallis and multi comparison test were used to determine statistical significance. *p < 0.05, **p < 0.01.

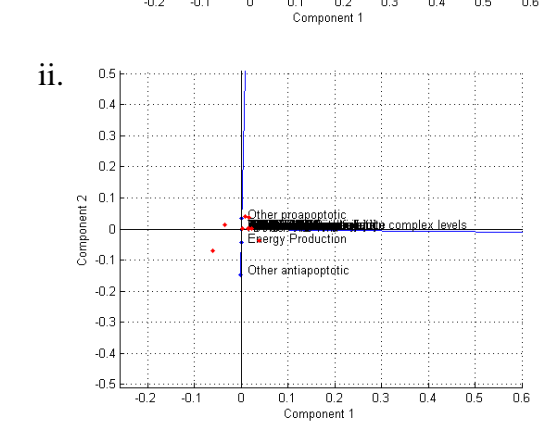
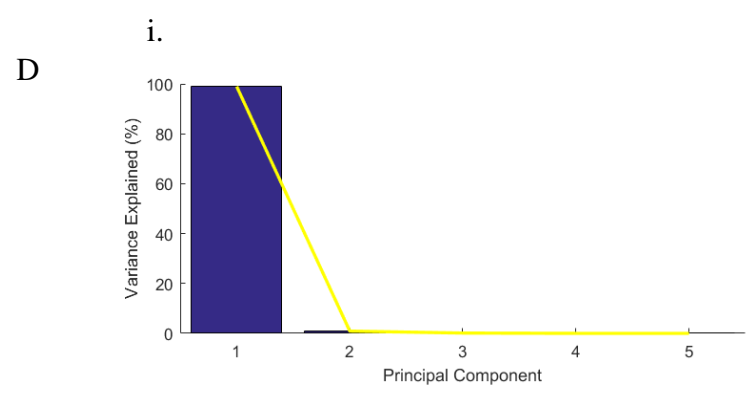
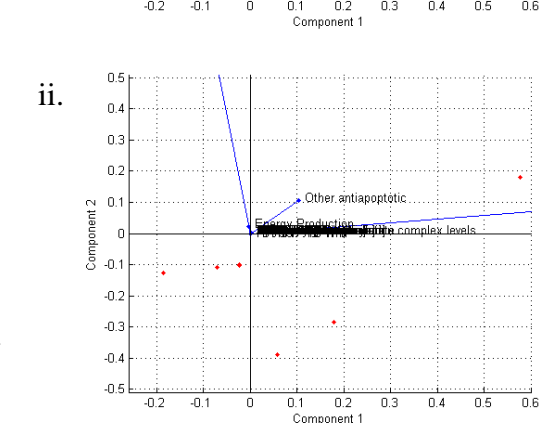
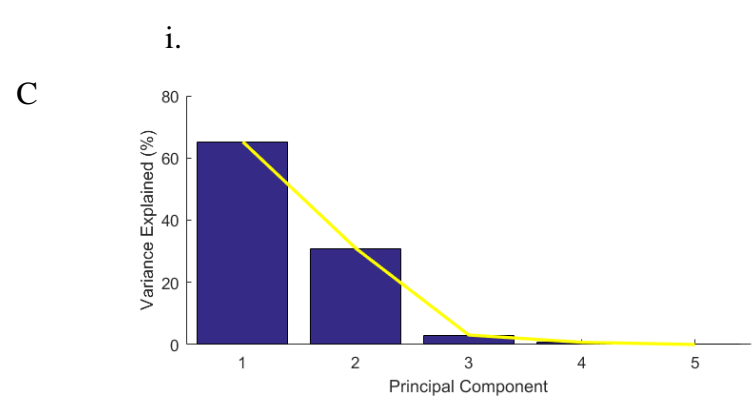
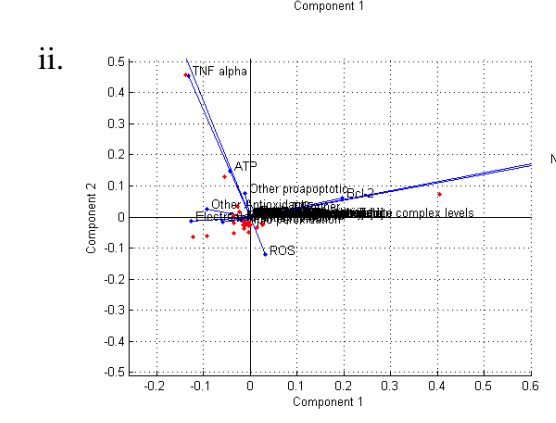
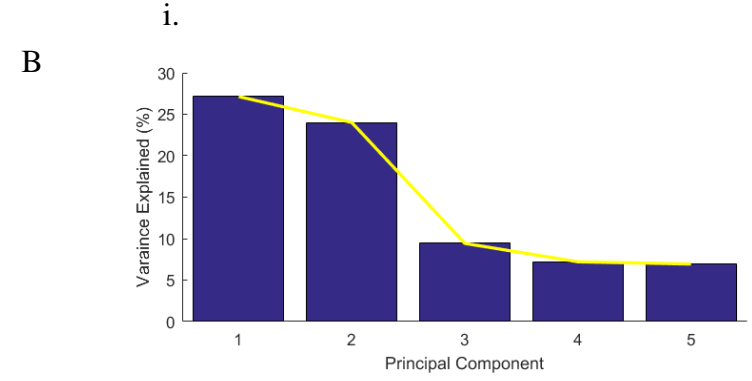
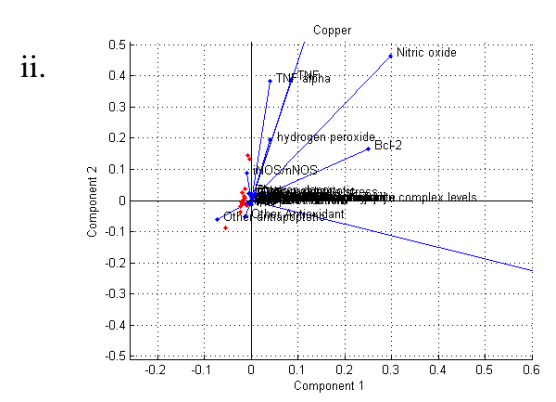
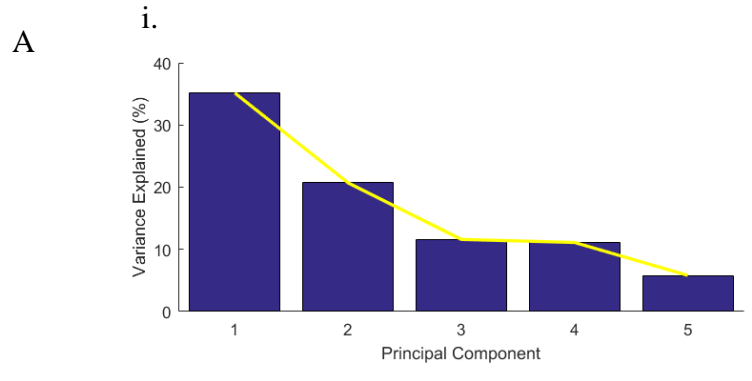


Figure 9. Principal component analysis (PCA) of individual metrics in G93A and WT mice. PCA analysis performed on the datasets containing metrics influencing disease progression for both WT and SOD1 G93A *in vitro* and *in vivo* data. Scree plots for each mouse type and projection of metrics onto first and second principal components were created. *A.* WT *in vitro* data. Scree plot indicates that principal component 1, correlated most strongly with caspase-8 levels, accounted for 35.1% of the variance and principal component 2, correlated most strongly with copper levels, accounted for 20.7% of the variance. *B.* SOD1 G93A *in vitro* data. Scree plot indicates that principal component 1, correlated most strongly with caspase-8 levels, accounted for 27.1% of the variance and principal component 2, correlated most strongly with iNOS/nNOS levels, accounted for 24.0% of the variance. *C.* WT *in vivo* data. Scree plot indicates that principal component 1, correlated most strongly with other antioxidant levels, accounted for 65.3% of the variance and principal component 2, correlated most strongly with other oxidative stress levels, accounted for 31.0% of the variance. *D.* SOD1 G93A *in vivo* data. Scree plot indicates that principal component 1, correlated most strongly with other antioxidant levels, almost exclusively accounted for the variance observed (99.0%).

5.2 Regulatory Mechanisms in SOD1 G93A and Wild-type Mice: A Comparison

Throughout the analysis, we have discovered that the SOD1 G93A system responses to perturbations are inherently different from WT system responses. Perturbations from each of the categories to the WT system produce physiological responses, which initially deviate slightly from the pre-perturbation state, but eventually return to the initial and expected homeostatic state; moreover, the WT system has been shown to respond in a similar manner to perturbations throughout its lifespan. The WT system is able to effectively respond to perturbations because its regulatory mechanisms are able to efficiently compensate for perturbations without overzealously reacting, which would otherwise induce continuous oscillatory instability (akin to an engineered control system with a too-high gain). Ultimately, these regulatory mechanisms confer stability to the WT model, which provides adequate resistance to any harmful changes to the system.

In direct contrast to the WT model, the SOD1 G93A model has been shown in this analysis to respond more aggressively, with evidence of higher amplitude and more frequent fluctuations following perturbation. These observations are exemplified by the difference in magnitude and fold changes of the SOD1 G93A responses to perturbations, especially apoptosis- and oxidative stress-related ones. The SOD1 G93A behavior observed when the system is perturbed provides evidence in support of a phenomenon called “hypervigilant regulation.” It can be characterized as a tendency for regulatory mechanisms to correct disturbances to homeostasis

through exaggerated responses. [10, 11] Initially, the aggressive nature of the SOD1 G93A responses may not be detrimental to the viability of the system. However, over time, the repeated strain placed on the regulatory mechanisms to compensate for perturbations is believed to destabilize the system and contribute to the ALS phenotype. [9, 10] In short, the SOD1 G93A mouse model is akin to an engineered control system with a too-high gain. With small perturbations early in life, the SOD1 G93A mouse's overzealous control is not detrimental to its life or motor function. However, a larger single perturbation or multiple smaller perturbations puts the system at risk for disastrous instability, initiating the true "onset" of ALS and ultimately resulting in the propagation and spread of motoneuron death. Hypervigilant regulation could explain why clinical ALS patients tend to be "healthier" than the normal population early in their life; their over-zealous physiology aggressively corrects small imbalances that would otherwise result in diseases like hyperlipidemia, diabetes, or hypertension. Instead, as larger or cumulative perturbations are sustained later in life, the overzealous regulatory physiology cannot maintain homeostasis. Given motoneurons are inherently more susceptible to instability, they succumb to the disease and phenotype we see and know as ALS. [10, 11]

5.3 Role of Bioenergetics-Apoptosis-Oxidative Stress Triad in ALS System Instability.

Given the sensitivity of the SOD1 G93A model to apoptosis- and oxidative stress-related perturbations, and the resulting changes to the system in response to them, the broader categories of apoptosis and oxidative stress appear to play instrumental roles in ALS disease progression induced by synergistic and degenerate interaction. This conclusion is further confirmed by the results of the PCA analysis pinpointing caspase-8 and various oxidative stress metrics as being primary contributors to variance in the data. In addition, the study's findings suggest that apoptosis and oxidative stress contribute more to disease progression than bioenergetics. However, it is important to recognize that the bioenergetics data pool is considerably smaller than the apoptosis and oxidative stress data pools because fewer studies have been performed on bioenergetics-related metrics in relation to ALS. As a result, the effect of bioenergetics could be under-represented in both its magnitude of effect and degree of interaction. However, the experimental data does show that bioenergetics is consistently depressed in SOD1 G93A mice from birth, well before the onset of symptoms. The narrower range of bioenergetics parameters corresponding to stable steady-state solutions in the wild type mouse reveal that there is less

degeneracy and redundancy in the bioenergetics category. Therefore, it is more difficult for bioenergetics to compensate for perturbation even in the wild type mouse model. It appears the implicit impact of bioenergetics could be much greater on overall regulation and system stability, even if at the experimental single-metric level, it appears to be less directly tied to cell death than oxidative stress and apoptotic pathways. Moreover, both the statistical assessment of experimental data and the present computer models indicate that perturbations in the oxidative stress pathway initiate a death-spiral cascade in the SOD1 G93A mouse that precludes the pathophysiology from re-establishing homeostasis. Future work will be necessary to affirm this preliminary finding.

REFERENCES

- [1] T. S. Wingo, D. J. Cutler, N. Yarab, C. M. Kelly, and J. D. Glass, "The heritability of amyotrophic lateral sclerosis in a clinically ascertained United States research registry," *PLoS One*, vol. 6, no. 11, p. e27985, 2011.
- [2] S. R. Pfohl, M. T. Halicek, and C. S. Mitchell, "Characterization of the Contribution of Genetic Background and Gender to Disease Progression in the SOD1 G93A Mouse Model of Amyotrophic Lateral Sclerosis: A Meta-Analysis," *J Neuromuscul Dis*, vol. 2, no. 2, pp. 137-150, 2015.
- [3] R. B. Kim, Irvin, C. W., Tilva, K. R., Mitchell, C. S., "State of the field: An informatics-based systematic review of the SOD1-G93A amyotrophic lateral sclerosis transgenic mouse model," *Informa Healthcare*, April 2015 2015.
- [4] M. Mattiazzi *et al.*, "Mutated human SOD1 causes dysfunction of oxidative phosphorylation in mitochondria of transgenic mice," *J Biol Chem*, vol. 277, no. 33, pp. 29626-33, Aug 16 2002.
- [5] E. Pollari, G. Goldsteins, G. Bart, J. Koistinaho, and R. Giniatullin, "The role of oxidative stress in degeneration of the neuromuscular junction in amyotrophic lateral sclerosis," *Front Cell Neurosci*, vol. 8, p. 131, 2014.
- [6] M. T. Carri, C. Valle, F. Bozzo, and M. Cozzolino, "Oxidative stress and mitochondrial damage: importance in non-SOD1 ALS," *Front Cell Neurosci*, vol. 9, p. 41, 2015.
- [7] M. Li *et al.*, "Functional role of caspase-1 and caspase-3 in an ALS transgenic mouse model," *Science*, vol. 288, no. 5464, pp. 335-9, Apr 14 2000.
- [8] S. K. Hollinger, I. S. Okosun, and C. S. Mitchell, "Antecedent Disease and Amyotrophic Lateral Sclerosis: What Is Protecting Whom?," *Front Neurol*, vol. 7, p. 47, 2016.
- [9] C. S. a. L. Mitchell, R.H., "Dynamic Meta-Analysis as a Therapeutic Prediction Tool for Amyotrophic Lateral Sclerosis," in *Amyotrophic Lateral Sclerosis*, P. M. M. (Ed.), Ed.: InTech, 2012.
- [10] C. S. Mitchell, S. K. Hollinger, S. D. Goswami, M. A. Polak, R. H. Lee, and J. D. Glass, "Antecedent Disease is Less Prevalent in Amyotrophic Lateral Sclerosis," *Neurodegener Dis*, vol. 15, no. 2, pp. 109-13, 2015.
- [11] C. W. Irvin, R. B. Kim, and C. S. Mitchell, "Seeking homeostasis: temporal trends in respiration, oxidation, and calcium in SOD1 G93A Amyotrophic Lateral Sclerosis mice," *Front Cell Neurosci*, vol. 9, p. 248, 2015.
- [12] S. C. Barber, R. J. Mead, and P. J. Shaw, "Oxidative stress in ALS: a mechanism of neurodegeneration and a therapeutic target," *Biochim Biophys Acta*, vol. 1762, no. 11-12, pp. 1051-67, Nov-Dec 2006.
- [13] M. B. Bogdanov, L. E. Ramos, Z. Xu, and M. F. Beal, "Elevated "hydroxyl radical" generation in vivo in an animal model of amyotrophic lateral sclerosis," *J Neurochem*, vol. 71, no. 3, pp. 1321-4, Sep 1998.
- [14] P. Cassina *et al.*, "Mitochondrial dysfunction in SOD1G93A-bearing astrocytes promotes motor neuron degeneration: prevention by mitochondrial-targeted antioxidants," *J Neurosci*, vol. 28, no. 16, pp. 4115-22, Apr 16 2008.
- [15] H. Muyderman and T. Chen, "Mitochondrial dysfunction in amyotrophic lateral sclerosis - a valid pharmacological target?," *Br J Pharmacol*, vol. 171, no. 8, pp. 2191-205, Apr 2014.
- [16] E. D'Amico, P. Factor-Litvak, R. M. Santella, and H. Mitsumoto, "Clinical perspective on oxidative stress in sporadic amyotrophic lateral sclerosis," *Free Radic Biol Med*, vol. 65, pp. 509-27, Dec 2013.

- [17] M. T. Lin and M. F. Beal, "Mitochondrial dysfunction and oxidative stress in neurodegenerative diseases," *Nature*, vol. 443, no. 7113, pp. 787-95, Oct 19 2006.
- [18] R. Liu, B. Li, S. W. Flanagan, L. W. Oberley, D. Gozal, and M. Qiu, "Increased mitochondrial antioxidative activity or decreased oxygen free radical propagation prevent mutant SOD1-mediated motor neuron cell death and increase amyotrophic lateral sclerosis-like transgenic mouse survival," *J Neurochem*, vol. 80, no. 3, pp. 488-500, Feb 2002.
- [19] N. A. Reyes, J. K. Fisher, K. Austgen, S. VandenBerg, E. J. Huang, and S. A. Oakes, "Blocking the mitochondrial apoptotic pathway preserves motor neuron viability and function in a mouse model of amyotrophic lateral sclerosis," *J Clin Invest*, vol. 120, no. 10, pp. 3673-9, Oct 2010.
- [20] P. J. Shaw, "Molecular and cellular pathways of neurodegeneration in motor neurone disease," *J Neurol Neurosurg Psychiatry*, vol. 76, no. 8, pp. 1046-57, Aug 2005.
- [21] M. Cozzolino, A. Ferri, and M. T. Carri, "Amyotrophic lateral sclerosis: from current developments in the laboratory to clinical implications," *Antioxid Redox Signal*, vol. 10, no. 3, pp. 405-43, Mar 2008.
- [22] H. H. Szeto, "Mitochondria-targeted peptide antioxidants: novel neuroprotective agents," *AAPS J*, vol. 8, no. 3, pp. E521-31, Aug 18 2006.
- [23] J. H. a. L. Shin, J.K., "Multiple Routes of Motor Neuron Degeneration in ALS," in *Current Advances in Amyotrophic Lateral Sclerosis*, P. A. E. (Ed.), Ed.: InTech, 2013.
- [24] C. Raoul *et al.*, "Motoneuron death triggered by a specific pathway downstream of Fas. potentiation by ALS-linked SOD1 mutations," *Neuron*, vol. 35, no. 6, pp. 1067-83, Sep 12 2002.